Examination of Consistency of QRPA Approach to Double-Beta Decay

J. Terasaki

Institute of Experimental and Applied Physics, Czech Technical University in Prague, Horská 3a/22, 128 00, Prague 2, Czech Republic

Abstract

Determination of the neutrino mass scale is a major subject of modern physics. I calculate the nuclear matrix element of the neutrinoless double-β decay of ^{48}Ca and derive the reduced half-life, which makes a relation between the half-life and the effective neutrino mass. The nuclear wave functions are obtained by the quasiparticle random-phase approximation. The reduced half-life of a few nuclear species are shown along with those of other groups. My value of reduced half-life is much larger than the majority of values of other groups. The charge-change transition density is examined by comparing the calculated transition strength function with that extracted by the charge-change reactions. The data are reproduced successfully using the appropriate transition operator and my charge-change transition density.

Keywords: *Neutrinoless double-β decay; effective neutrino mass; nuclear matrix element; QRPA*

1 Introduction

Nuclear theory plays two indispensable roles in neutrino physics. One is a calculation of the cross section of the ν-nucleus scattering [1] in relation to the neutrino-oscillation experiments, and another is a calculation of the nuclear matrix element (NME) and phase-space factor of the neutrinoless double-β ($0\nu\beta\beta$) decay for determining the effective neutrino mass. The half-life of this decay is a function of the NME, phase-space factor, and the effective neutrino mass, thus, a reliable predictive calculation of these theoretical quantities are necessary. ^{48}Ca is the lightest candidate of the mother nuclei for the experiments. The nuclear wave functions cannot be obtained without an approximation. On the other hand, the values of the phase-space factor are established for relatively light candidate nuclei because accurate wave functions of the emitted particles can be used. It is a well-known problem that the calculated NME of the $0\nu\beta\beta$ decay is distributed in a region of a factor of 2–3 systematically depending on the theoretical methods [2]. The number of calculations increased in the past decade, however this uncertainty factor does not change. The NME also affects the future plans of the experimental facilities for observing the $0\nu\beta\beta$ decay

Proceedings of the International Conference 'Nuclear Theory in the Supercomputing Era — 2018' (NTSE-2018), Daejeon, South Korea, October 29 – November 2, 2018, eds. A. M. Shirokov and A. I. Mazur. Pacific National University, Khabarovsk, Russia, 2019, p. 100.

http://www.ntse.khb.ru/files/uploads/2018/proceedings/Terasaki.pdf.

because the NME affects an amount of the detector materials necessary for the aimed effective neutrino masses [3].

The reason for the discrepancy of the calculated NMEs is not yet clarified. The shell model includes high-order particle-hole correlations, but the single-particle space is limited to one major shell in most of the calculations. The quasiparticle random-phase approximation is not constrainted by this limit, but its applicability is limited to nuclei in which the effects of high-order particle-hole correlations are small. Under this circumstance, the appropriate effective g_A, the axial-vector current coupling, is not yet established. Thus, the key point of the NME study is how the reliability of the calculation is shown.

Operators for calculating the $0\nu\beta\beta$ NME are the neutrino potential and the charge-change operators of the Gamow–Teller (GT), Fermi, and the tensor types. The last one has only a small contribution, and it is neglected in my calculations. The GT transition density associated with $J^\pi = 1^+$ is an ingredient of the NME calculation. This transition density is also included in the charge-change strength function, which can be extracted from the experimental cross sections using the impulse approximation and an extrapolation to the limit of vanishing momentum transfer [4]. There are experimental charge-change strength functions obtained in this manner from the $^{48}\mathrm{Ca}(p,n)^{48}\mathrm{Sc}$ and $^{48}\mathrm{Ti}(n,p)^{48}\mathrm{Sc}$ reactions [5]. In this paper, I show that these data can be reproduced by my QRPA calculation. However, this reproduction is not trivial because the experimental data do not satisfy the GT sum rule. This problem is resolved by introducing an isovector spin-monopole operator in addition to the usual GT operator. By this test, the validity of my charge-change transition density is proven indirectly.

2 Nuclear matrix element of neutrinoless double-β decay

The effective neutrino mass is defined by

$$\langle m_\nu \rangle = \left| \sum_{i=1,2,3} U_{ei}^2 \, m_i \right|, \tag{1}$$

where U_{ei} is the matrix element of the Pontecorvo–Maki–Nakagawa–Sakata (PMNS) matrix [6] with i denoting the eigenstate of mass m_i. Suffix e stands for the electron flavor. The half-life to the $0\nu\beta\beta$ decay $T_{1/2}^{(0\nu)}$ and $\langle m_\nu \rangle$ are related as [7]

$$T_{1/2}^{(0\nu)} = \frac{R_{1/2}^{(0\nu)}}{\langle m_\nu \rangle^2}, \tag{2}$$

$$R_{1/2}^{(0\nu)} = \frac{(m_e c^2)^2}{G_{0\nu}\, g_A^4 |M^{(0\nu)}|^2}, \tag{3}$$

where $G_{0\nu}$ is the phase-space factor, g_A is the axial-vector current coupling, $M^{(0\nu)}$ is the NME, and m_e is the electron mass. I call $R_{1/2}^{(0\nu)}$ a reduced half-life.

The $0\nu\beta\beta$-decay NME $M^{(0\nu)}$ is obtained by calculating

$$M^{(0\nu)} = M_{GT}^{(0\nu)} - \frac{g_V^2}{g_A^2} M_F^{(0\nu)}. \tag{4}$$

$M^{(0\nu)}_{GT}$ is the GT NME, and $M^{(0\nu)}_{F}$ is the Fermi NME. The vector current coupling g_V is 1; this coupling is thought to be a physical constant. An effective value is used for g_A (see below). Those NMEs can be written as

$$M^{(0\nu)}_{GT} = \sum_K \sum_{a^K_I a^K_F} \sum_{pnp'n'} V^{GT(0\nu)}_{pp',nn'}(\bar{E}_a) \langle F|c^\dagger_p c_n|a^K_F\rangle\langle a^K_F|a^K_I\rangle\langle a^K_I|c^\dagger_{p'}c_{n'}|I\rangle, \tag{5}$$

$$M^{(0\nu)}_{F} = \sum_K \sum_{a^K_I a^K_F} \sum_{pnp'n'} V^{F(0\nu)}_{pp',nn'}(\bar{E}_a) \langle F|c^\dagger_p c_n|a^K_F\rangle\langle a^K_F|a^K_I\rangle\langle a^K_I|c^\dagger_{p'}c_{n'}|I\rangle. \tag{6}$$

The initial and final states of the $0\nu\beta\beta$ decay are denoted by $|I\rangle$ and $|F\rangle$, respectively, and the states of the intermediate nucleus are $|a^K_F\rangle$ and $|a^K_I\rangle$. The states $\{|a^K_F\rangle\}$ are obtained by QRPA[1] based on $|F\rangle$, and $\{|a^K_I\rangle\}$ are obtained by QRPA based on $|I\rangle$. K is a component of the nuclear angular momentum projected on the symmetry axis; in my calculation, the axial symmetry of the nuclear density distribution is assumed. The indexes p and p' denote the proton states, and n and n' denote the neutron states. $c^\dagger_i$ and c_i are respectively the creation and annihilation operators of a particle in the state i. $\langle F|c^\dagger_p c_n|a^K_F\rangle$ and $\langle a^K_I|c^\dagger_{p'}c_{n'}|I\rangle$ are the transition-density matrices of the charge change. $V^{GT(0\nu)}_{pp',nn'}(\bar{E}_a)$ and $V^{F(0\nu)}_{pp',nn'}(\bar{E}_a)$ are the two-body transition matrix elements:

$$V^{GT(0\nu)}_{pp',nn'}(\bar{E}_a) = \langle pp'|h_+(r_{12},\bar{E}_a)\,\boldsymbol{\sigma}(1)\cdot\boldsymbol{\sigma}(2)\,\tau^-(1)\,\tau^-(2)|nn'\rangle, \tag{7}$$

$$V^{F(0\nu)}_{pp',nn'}(\bar{E}_a) = \langle pp'|h_+(r_{12},\bar{E}_a)\,\tau^-(1)\,\tau^-(2)|nn'\rangle. \tag{8}$$

The operators of the spin and charge change from neutron to proton are denoted by $\boldsymbol{\sigma}$ and τ^-, respectively. Their argument distinguishes the two particles that the operators act on. The neutrino potential is given by

$$h_+(r_{12},\bar{E}_a) \simeq \frac{R}{r_{12}}\frac{2}{\pi}\Big\{\sin\Big(\frac{c}{\hbar}\bar{\mu}_a m_e r_{12}\Big)\,\mathrm{ci}\Big(\frac{c}{\hbar}\bar{\mu}_a m_e r_{12}\Big) \tag{9}$$

$$-\cos\Big(\frac{c}{\hbar}\bar{\mu}_a m_e r_{12}\Big)\,\mathrm{si}\Big(\frac{c}{\hbar}\bar{\mu}_a m_e r_{12}\Big)\Big\}, \tag{10}$$

$$\bar{\mu}_a = \frac{1}{m_e c^2}(\bar{E}_a - \bar{M}). \tag{11}$$

This neutrino potential is derived by neglecting the effective neutrino mass compared to the major momentum transfer by the propagating neutrino [7]. R is the root-mean-square radius of nucleus, r_{12} is the distance variable between two particles, and $\bar{E}_a$ is the average energy of the intermediate states (the closure approximation). $R = 1.1\,A^{1/3}$ fm with the mass number A and $\bar{\mu}_a = 18.51$ [7] are used in our calculations. In Eq. (10), the functions

$$\mathrm{si}(x) = -\int_x^\infty \frac{\sin(t)}{t}\,dt, \qquad \mathrm{ci}(x) = -\int_x^\infty \frac{\cos(t)}{t}\,dt \tag{12}$$

are used.

The interaction used for obtaining the nuclear states is the Skyrme SkM* [9] and volume contact pairing interactions. The QRPA equation was solved in the matrix

[1]The proton-neutron QRPA [8] is used. I call it the QRPA for simplicity in this paper.

Table 1: NME of $0\nu\beta\beta$ decay of ^{48}Ca, specific terms, effective g_A used for the calculation, and reduced half-life.

$M^{(0\nu)}$	$M^{(0\nu)}_{GT}$	$M^{(0\nu)}_{F}$	g_A	$R^{(0\nu)}_{1/2}$ (10^{12} MeV^2 yr)
3.054	1.723	−0.319	0.49	19.572

formulation. Table 1 shows the obtained NME, GT and Fermi terms, effective g_A, and the reduced half-life of the $0\nu\beta\beta$ decay of ^{48}Ca. The effective $g_A = 0.49$ was determined so as to reproduce the measured half-life to the $2\nu\beta\beta$ decay [10]. This value of g_A is much smaller than the bare value of approximately 1.27. Figure 1

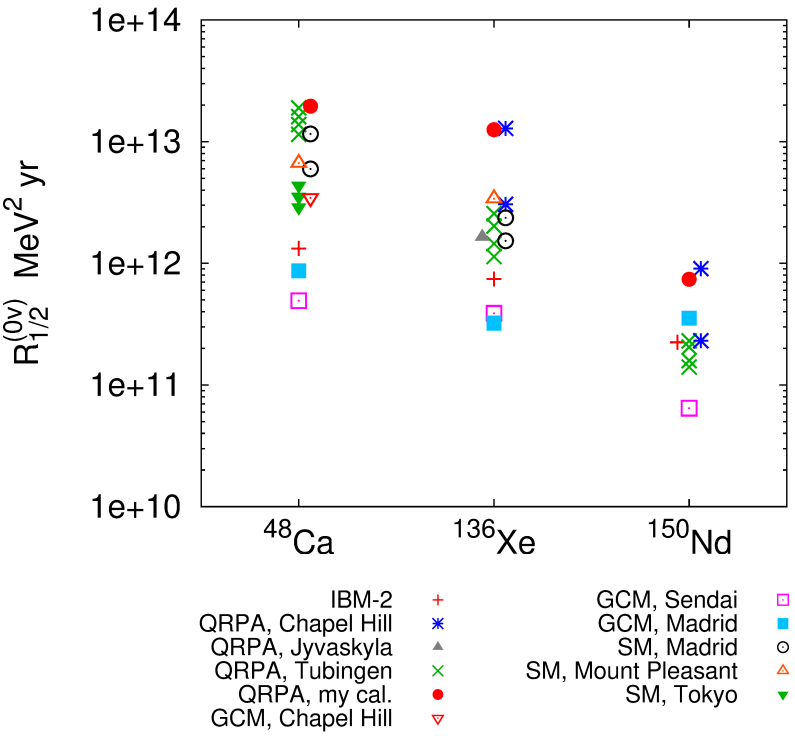

Figure 1: Reduced half-life of ^{48}Ca, ^{136}Xe, and ^{150}Nd obtained by several groups. The references are as follows. ^{48}Ca: [11] (QRPA Tübingen), [12] (SM, Mount Pleasant), [13] (SM, Tokyo), [14] (IBM-2), [15] (GCM, Madrid), [16] (GCM, Sendai), [17] (SM, Madrid), [18] (GCM, Chapel Hill), [19] (QRPA, my calculation); ^{136}Xe: [14] (IBM-2), [11] (QRPA, Tübingen), [20] (QRPA, Chapel Hill), [16] (GCM, Sendai), [15] (GCM, Madrid), [17] (SM, Madrid), [12] (SM, Mount Pleasant), [21] (QRPA, Jyväskylä), [22] (QRPA, my calculation); ^{150}Nd: [14] (IBM-1), [23] (QRPA, Tübingen), [20] (QRPA, Chapel Hill), [16] (GCM, Sendai), [15] (GCM, Madrid), [24, 25] (QRPA, my calculation). SM, GCM, and IBM stand for the shell model, generator coordinate method, and interacting boson model, respectively. The effective g_A is not unified.

illustrates the reduced half-life of three nuclear species obtained by several groups including my values, which are much higher than the majority of the results of other groups. This result implies that the half-life is predicted by my calculation to be much longer than that of other groups. Test of reliability of my calculation is quite important.

3 Charge-change strength function

The experimental GT strength function of ^{48}Ca$(p,n)^{48}$Sc and GT$^+$ [$\tau^+ = (\tau^-)^\dagger$ is used] strength function of ^{48}Ti$(n,p)^{48}$Sc are drawn in Fig. 2 together with my theoretical strength functions obtained by calculating

$$S_{\mathrm{GT}^-}(E) = \frac{1}{\pi}\sum_{a_I^K}\frac{\delta|\langle a_I^K|\boldsymbol{\sigma}\tau^-|I\rangle|^2}{[E-E(a_I^K)]^2+\delta^2}. \tag{13}$$

$E(a_I^K)$ is the energy of the state $|a_I^K\rangle$, and δ is a small constant for smoothing. The transition operator $\boldsymbol{\sigma}\tau^-$ is the one-body operator. The summation includes all states of ^{48}Sc for which the transition matrix element does not vanish. The GT$^+$ strength function can be calculated analogously using $|F\rangle$ and $|a_F^K\rangle$. The calculated strength functions apparently overestimate the data, however these results satisfy the GT sum rule,

$$\int_0^\infty dE\, S_{\mathrm{GT}^-}(E)|_{(Z,N)\to(Z+1,N-1)} - \int_0^\infty dE\, S_{\mathrm{GT}^+}(E)|_{(Z,N)\to(Z-1,N+1)} = 3(N-Z). \tag{14}$$

For the initial nucleus ^{48}Ca, the first term provides the value of 24.638 while the second term is equal to -0.633 resulting in the sum-rule value of 24.005. For the initial nucleus ^{48}Ti, I obtain respectively 15.257 and -3.268 and thus the value of 11.989 for the sum rule. The exact values are respectively 24 and 12 for these two nuclei. The sum of the experimental charge-change transition strengths of ^{48}Ca$(p,n)^{48}$Sc

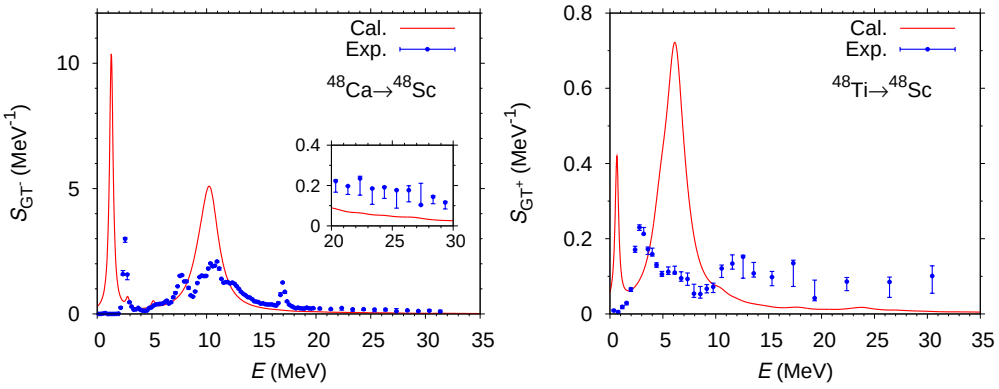

Figure 2: Charge-change strength functions of ^{48}Ca$(p,n)^{48}$Sc (left) and ^{48}Ti$(n,p)^{48}$Sc (right). Symbols are the experimental data of Ref. [5], solid lines are the results of my calculations. The inset in the left panel is a magnification of the high-energy region.

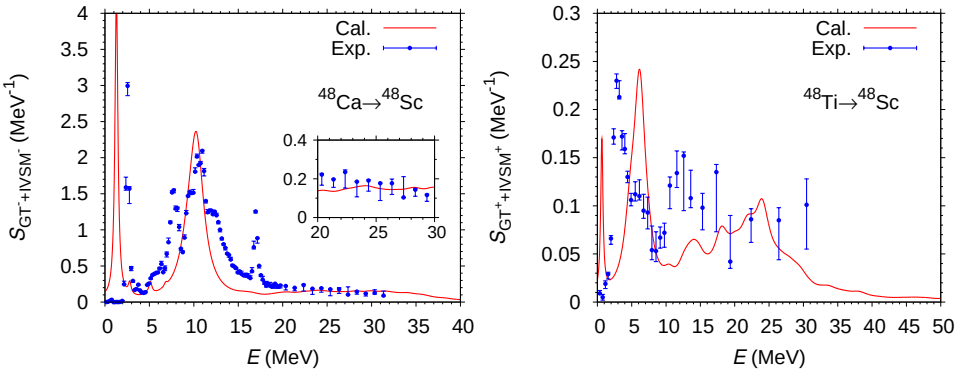

Figure 3: The same as Fig. 2 but for the transition operator $O_{\pm}$.

is 64 ± 9 % of the sum-rule [5]. The tail of the experimental strength function (left panel of Fig. 2) converges to zero, indicating that there is no strength in the higher-energy region. Thus, it is implied by the data, that this transition involves not only the GT operator $\boldsymbol{\sigma}\tau^-$ but also other ones. A possible candidate is the isovector spin-monopole operator $r^2\boldsymbol{\sigma}\tau^-$ [26,27]. This operator causes a two-$\hbar\omega$ jump and can explain the strength distribution in the higher-energy region where $\boldsymbol{\sigma}\tau^-$ cannot create the strength, see the right panel in Fig. 2. The possible contribution of the isovector spin-monopole operator has been already mentioned in Ref. [5].

I introduce the transition operator [19]

$$O_{\pm} = \boldsymbol{\sigma}\tau^{\pm} + \alpha_{\pm} r^2 \boldsymbol{\sigma}\tau^{\pm}, \tag{15}$$

and determine $\alpha_{\pm}$ so as to reproduce the experimental strength functions in the two-$\hbar\omega$-jump region; those values are $\alpha_- = -0.03$ fm^{-2} for ^{48}Ca $\to$ ^{48}Sc and $\alpha_+ = -0.0253$ fm^{-2} for ^{48}Ti $\to$ ^{48}Sc. The strength functions of $O_{\pm}$ are drawn in Fig. 3 together with the experimental data. The description of the data is improved significantly. Therefore, the contribution of the isovector spin-monopole operator is a reasonable explanation to the observed charge-change transitions. It is stressed that my transition density is confirmed indirectly through this reproduction of the data.

The calculated strength function of $O_{\pm}$ up to 12 MeV (^{48}Ca) or 10 MeV (^{48}Ti) is lowered compared to that of the GT operator. This change can be understood by rewriting $O_{\pm}$ as

$$O_{\pm} = \left\{1 + \alpha_{\pm}\langle r^2\rangle_{nf_{7/2}} + \alpha_{\pm}(r^2 - \langle r^2\rangle_{nf_{7/2}})\right\}\boldsymbol{\sigma}\tau^{\pm}, \tag{16}$$

where $\langle r^2\rangle_{nf_{7/2}}$ is the expectation value of r^2 with respect to the specified neutron state. The operator $\alpha_{\pm}(r^2 - \langle r^2\rangle_{nf_{7/2}})$ is the two-$\hbar\omega$ component in a good approximation [27]. Since $\alpha_{\pm}$ are negative, the zero-$\hbar\omega$ component $1 + \alpha_{\pm}\langle r^2\rangle_{nf_{7/2}}$ is hindered.

4 Summary

I have calculated the NME of the $0\nu\beta\beta$ decay of ^{48}Ca $\to$ ^{48}Ti using the QRPA, and the reduced half-life was obtained. My result predicts much longer half-life of ^{48}Ca to that decay compared to those predicted by other groups. Check of the transition

density has been made indirectly by reproducing the charge-change strength functions obtained by the (n,p) and (p,n) reactions. As a by-product, it has been shown that the transition operator of that charge-change reaction includes the isovector spin-monopole operator.

In this paper, I omitted the discussions on the two-neutrino double-β ($2\nu\beta\beta$) decay and the detail of the method to determine the strength of the proton-neutron (pn) pairing interaction [19]. The strength of the isoscalar pn pairing interaction is determined by an identity derived under the closure approximation, and the effective g_A is determined so as to reproduce the measured half-life to the $2\nu\beta\beta$ decay. The convergence of the $0\nu\beta\beta$ NME was also checked with respect to the single-particle space. Thus, my calculation does not have a free parameter.

Acknowledgments

Numerical calculations of this paper were performed by the K computer at the RIKEN Center for Computational Science through the program of High Performance Computing Infrastructure in 2017−2018 and 2018−2019 (hp170288). The computer Coma at the Center for Computational Sciences, University of Tsukuba was also used through the Multidisciplinary Cooperative Research Program of this center in 2016 (TKBNDFT) and 2017 (DBTHEORY). Furthermore, the computer Oakforest-PACS at the Joint Center for Advanced High Performance Computing was used through the above program of the Center for Computational Sciences, University of Tsukuba in 2018 (xg18i006). This study is supported by the European Regional Development Fund-Project "Engineering applications of microworld physics" (No. CZ.02.1.01/0.0/0.0/16_019/0000766).

References

[1] C. Barbieri, *Recent (computational and non) advances for self-consistent Green's function theory in nuclear physics*, talk given at the Int. Conf. 'Nuclear Theory in the Supercomputing Era — 2018' (NTSE-2018), October 29 – November 2, 2018, Daejeon, South Korea, http://ntse.khb.ru/files/uploads/2018/presentations/Barbieri.pdf.

[2] J. Engel and J. Menéndez, Rep. Prog. Phys. **80**, 046301 (2017).

[3] A. S. Barabash, Front. Phys., **6**,160 (2019).

[4] M. Ichimura, H. Sakai and T. Wakasa, Prog. Part. Nucl. Phys. **56**, 446 (2006).

[5] K. Yako *et al.*, Phys. Rev. Lett. **103**, 012503 (2009).

[6] B. Pontecorvo, Sov. Phys. JETP **7**, 172 (1958).

[7] M. Doi, T. Kotani and E. Takasugi, Prog. Theor. Phys. Suppl. **83**, 1 (1985).

[8] J. A. Halbleib Sr. and R. A. Sorensen, Nucl. Phys. A **98**, 542 (1967).

[9] J. Bartel, P. Quentin, M. Brack, C. Guet and H.-B. Håkansson, Nucl. Phys. A **386**, 79 (1982).

[10] A. S. Barabash, in *Proc. Workshop on Calculation of Double-Beta-Decay Matrix Elements (MEDEX'13), Prague, June 11–14, 2013*, eds. O. Civitarese, I. Stekl and J. Suhonen. AIP Publishing, 2013, p. 11.

[11] F. Šimkovic, V. Rodin, A. Faessler and P. Vogel, Phys. Rev. C **87**, 045501 (2013).

[12] M. Horoi and A. Neacsu, Phys. Rev. C **93**, 024308 (2016).

[13] Y. Iwata, N. Shimizu, T. Otsuka, Y. Utsuno, J. Menéndez, M. Homma and T. Abe, Phys. Rev. Lett. **116**, 112502 (2016).

[14] J. Barea, J. Kotila and F. Iachello, Phys. Rev. C **91**, 034304 (2015).

[15] N. L. Vaquero, T. R. Rodríguez and J. L. Egido, Phys. Rev. Lett. **111**, 142501 (2013).

[16] J. M. Yao, L. S. Song, K. Hagino, P. Ring and J. Meng, Phys. Rev. C **91**, 024316 (2015).

[17] J. Menéndez, A. Poves, E. Caurier and F. Nowacki, Nucl. Phys. A **818**, 139 (2009).

[18] C. F. Jiao, J. Engel and J. D. Holt, Phys. Rev. C **96**, 054310 (2017).

[19] J. Terasaki, Phys. Rev. C **97**, 034304 (2018).

[20] M. T. Mustonen and J. Engel, Phys. Rev. C **87**, 064302 (2013).

[21] J. Hyvärinen and J. Suhonen, Phys. Rev. C **91**, 024613 (2015).

[22] J. Terasaki and Y. Iwata, Phys. Rev. C **100**, 034325 (2019).

[23] D.-L. Fang, A. Faessler and F. Šimkovic, Phys. Rev. C **92**, 044301 (2015).

[24] J. Terasaki, Phys. Rev. C **91**, 034318 (2015).

[25] J. Terasaki, Phys. Rev. C **93**, 024317 (2016).

[26] O. Civitarese and J. Suhonen, Phys. Rev. C **89**, 044319 (2014).

[27] I. Hamamoto and H. Sagawa, Phys. Rev. C **62**, 024319 (2000).